Monthly Notices
of the
ROYAL ASTRONOMICAL SOCIETY

MNRAS **436,** 136–149 (2013)
Advance Access publication 2013 September 28

doi:10.1093/mnras/stt1541

No compelling evidence of significant early star cluster disruption in the Large Magellanic Cloud

Richard de Grijs,[1,2]★ Simon P. Goodwin[3] and Peter Anders[1,4]

[1]*Kavli Institute for Astronomy and Astrophysics, Peking University, Yi He Yuan Lu 5, Hai Dian District, Beijing 100871, China*
[2]*Department of Astronomy, Peking University, Yi He Yuan Lu 5, Hai Dian District, Beijing 100871, China*
[3]*Department of Physics & Astronomy, The University of Sheffield, Hicks Building, Hounsfield Road, Sheffield S3 7RH, UK*
[4]*Key Laboratory for Optical Astronomy, National Astronomical Observatories, Chinese Academy of Sciences, 20A Datun Road, Chaoyang District, Beijing 100012, China*

Accepted 2013 August 14. Received 2013 August 13; in original form 2013 May 17

ABSTRACT

Whether or not the rich star cluster population in the Large Magellanic Cloud (LMC) is affected by significant disruption during the first few $\times\ 10^8$ yr of its evolution is an open question and the subject of significant current debate. Here, we revisit the problem, adopting a homogeneous data set of broad-band imaging observations. We base our analysis mainly on two sets of self-consistently determined LMC cluster ages and masses, one using standard modelling and one which takes into account the effects of stochasticity in the clusters' stellar mass functions. On their own, the results based on any of the three complementary analysis approaches applied here are merely indicative of the physical conditions governing the cluster population. However, the combination of our results from all three different diagnostics leaves little room for any conclusion other than that the optically selected LMC star cluster population exhibits no compelling evidence of significant disruption – for clusters with masses, $M_{\rm cl}$, of $\log(M_{\rm cl}/{\rm M}_\odot) \gtrsim 3.0$–$3.5$ – between the age ranges of [3–10 and 30–100] Myr, either 'infant mortality' or otherwise. In fact, there is no evidence of any destruction beyond that expected from simple models just including stellar dynamics and stellar evolution for ages up to 1 Gyr. It seems, therefore, that the difference in environmental conditions in the Magellanic Clouds on the one hand and significantly more massive galaxies on the other may be the key to understanding the apparent variations in cluster disruption behaviour at early times.

Key words: galaxies: evolution – galaxies: individual: Large Magellanic Cloud – Magellanic Clouds – galaxies: star clusters: general.

1 INTRODUCTION

Star clusters are the most highly visible stellar population components in galaxies beyond the Local Group. Their integrated properties are generally used to trace, e.g., their host galaxy's star (cluster) formation history, the impact and time-scales of the most recent (major) mergers or close encounters with any neighbouring galaxies, and the extent to which environmental conditions drive the evolution of star cluster systems in their own right.

The galaxies in the Local Group represent unique benchmarks which can be used to verify analyses based on integrated cluster properties using resolved stellar photometry (e.g. de Grijs & Anders 2006; Colucci & Bernstein 2012; Baumgardt et al. 2013; Cezario et al. 2013; de Meulenaer et al. 2013). As such, the star cluster systems in the Small and Large Magellanic Clouds (SMC, LMC) can provide unique insights into the properties of their resolved star cluster populations. Prompted by recent claims (Chandar, Fall & Whitmore 2010a; Chandar, Whitmore & Fall 2010b) and counter-claims (e.g. Baumgardt et al. 2013) that the disruption rate of star clusters in the LMC may be significant from early ages (a few Myr) up to an age of ∼1 Gyr, we decided to revisit this issue based on a number of complementary approaches.

Chandar et al. (2010a,b) determined the cluster population's age and mass distributions based on fits to the broad-band spectral energy distributions (SEDs) from Hunter et al.'s (2003) comprehensive data base of integrated LMC cluster photometry. They used simple stellar population (SSP) models characterized by fully sampled stellar mass functions (MFs) for their parameter derivation (cf. Section 2). Two other studies used exactly the same photometric data base to independently determine the clusters' ages and masses. Specifically, de Grijs & Anders (2006) adopted fully sampled SSP models to determine the LMC cluster population's properties, while Popescu, Hanson & Elmegreen (2012) took into account the effects of stochastically sampled stellar MFs, which become particularly noticeable for cluster masses below a few $\times\ 10^4\ {\rm M}_\odot$ (cf. Section 3).

★E-mail: grijs@pku.edu.cn

Given that these studies all used the same basic cluster photometry, it is instructive to first compare Chandar et al.'s (2010a,b) results with those of de Grijs & Anders (2006), since both teams based their parameter determinations on the same underlying physical assumptions (barring small differences between the actual SSP models used, which we discuss below where relevant). We will then proceed by properly taking into account the effects of stochastic sampling of the clusters' stellar MFs, which is arguably a physically sounder assumption for lower mass clusters.

This debate goes beyond the mere niche of the question as to how star cluster populations evolve. Most importantly, it touches upon the process in which disrupting star clusters populate their host galaxy's galactic field. At present, two competing theories hold sway in this area. One supports the idea that early star cluster disruption is independent of the cluster mass and does not depend on the clusters' environment either (e.g. Chandar et al. 2010a,b; Fall & Chandar 2012), which must be contrasted with the view that environmental differences lead to different cluster disruption signatures, which may also exhibit a dependence on the cluster mass (e.g. de Grijs & Goodwin 2008, 2009, and references therein; see also Lamers 2009). In this paper, we will show that, at least for the LMC and for the data set in common among all competing studies (Hunter et al. 2003; de Grijs & Anders 2006; Chandar et al. 2010a,b; Popescu et al. 2012; Baumgardt et al. 2013), the overwhelming evidence rules out – at high statistical significance – substantial cluster disruption at early times ($t \lesssim 10^8$ yr). In Section 6.1, we will place these results in a more general context.

2 CLUSTER DATA

In de Grijs & Anders (2006), we compared the physical parameters of the LMC's star cluster population obtained from resolved photometry and spectroscopy on the one hand and integrated SEDs on the other. This was necessarily restricted to age comparisons of the more massive LMC sample clusters, as constrained by the availability of prior age determinations in the literature at that time. Using our ANALYSED tool for star cluster analysis based on broad-band SEDs assuming fully populated stellar MFs (Anders et al. 2004b), we re-analysed the current most comprehensive data base of integrated LMC cluster photometry (Hunter et al. 2003).

Prior to this, we had already concluded (de Grijs et al. 2005) that application of the ANALYSED approach based on standard modelling employing the GALEV SSP models (Kotulla et al. 2009, and references therein, as well as subsequent, unpublished updates) showed that the *relative* masses within a given cluster system can be determined to very high accuracy (provided that the clusters' stellar MFs are well populated), depending on the specific combination of passbands used (Anders et al. 2004b). Under the conditions explored in de Grijs et al. (2005), we found that the *absolute* accuracy with which the cluster mass distribution can be reproduced using different model approaches (including different SSP models, filter combinations and input physics) is $\sigma_M = \Delta\langle\log(M_{\rm cl}/{\rm M}_\odot)\rangle \leq 0.14$, compared with $\sigma_t = \Delta\langle\log(t\,{\rm yr}^{-1})\rangle \leq 0.35$ for the age distribution: '[t]his implies that mass determinations are mostly insensitive to the approach adopted' (de Grijs et al. 2005), because the mass-to-light ratio of a given SSP depends only weakly on the population's age, at least within reasonably narrow age ranges. In any cluster analysis used to derive ages and masses, the age uncertainties are, by far, the most significant.

Driven by a number of controversies that had appeared in the literature (Chandar, Fall & Whitmore 2006; Gieles, Lamers & Portegies Zwart 2007), we proceeded to apply our analysis approach to the SMC's star cluster system (de Grijs & Goodwin 2008), based on Hunter et al.'s (2003) broad-band magnitudes. We concluded that the optically selected SMC star cluster population has undergone at most ∼30 per cent disruption between the age ranges of approximately [3–10 and 40–160] Myr, a process often referred to as 'infant mortality'.[1] We ruled out an alleged (Chandar et al. 2006) 90 per cent cluster disruption rate per decade of $\log(t\,{\rm yr}^{-1})$ for $t \leq 10^9$ yr.

In the meantime, Chandar et al. (2010a,b) have used the same Hunter et al. (2003) photometric data base, combined with their independently determined yet unpublished age and mass estimates for 854 LMC clusters, to raise a new controversy. They suggest that a scenario in which clusters undergo gradual, mass-independent disruption up to $t \sim 1$ Gyr provides the best match to the data. However, Baumgardt et al. (2013) recently concluded that significant cluster disruption appears to set in only after an age of ∼200 Myr (see also de Grijs & Goodwin 2009). This latter conclusion is consistent with the results of Parmentier & de Grijs (2008). Neither of these latter authors focused on the evolution of the youngest clusters, however, nor did Baumgardt et al. (2013) explore the apparent discrepancies with Chandar et al. (2010a,b) in detail. Addressing these two aspects is what we set out to do here.

In addition, upon close inspection of the LMC cluster data base (which was kindly provided by D. Hunter), it turns out that it includes a significant number of duplicate clusters. These duplicates were not in all cases identified by Hunter et al. (2003), but they only become apparent based on a detailed comparison of the spatial distribution of the clusters. We hence proceeded to clean the Hunter et al. (2003) data base, resulting in a sample of 748 unique clusters (see also Popescu, Hanson & Elmegreen 2012; Baumgardt et al. 2013).

Fig. 1(a) shows the LMC cluster distribution in the diagnostic age–mass diagram based on our cleaned data base; the relevant cluster parameters are included in Table 1. The original integrated cluster photometry is available from Popescu et al. (2012, their tables 1 and 2). At first glance, two narrow features in the age distribution are apparent. These so-called chimneys at $\log(t\,{\rm yr}^{-1}) = 6.6$ and ∼7.2 are associated with, respectively, the minimum age included in our SSP models (any clusters characterized by younger SEDs are returned to the youngest age by our fitting routines) and the onset of red supergiants in realistic stellar populations. The latter chimney is an artefact caused by a local minimum in parameter space. We also note that the observational completeness limit (indicated by the solid red line, which represents the ∼50 per cent completeness level, at $M_V \simeq -4.3$ mag; for a discussion, see de Grijs & Anders 2006) is a function of age, so that – depending on the age range of interest – one needs to vary the minimum mass to compare and assess the MFs of different cluster subsamples.

Finally, we explored whether any other existing data bases of LMC cluster parameters could be exploited to support the analysis presented in this paper. We specifically focused on the catalogue of Glatt, Grebel & Koch (2010), who compiled data of 1193 populous LMC clusters with ages of up to 1 Gyr based on the most up-to-date and comprehensive LMC object catalogue of Bica et al. (2008). Glatt et al. (2010) used the optical broad-band photometry from the Magellanic Clouds Photometric Survey (MCPS;

[1] When we refer to 'infant' mortality in this paper, this relates to the mass-independent disruption of a fraction of the total cluster sample owing to rapid gas expulsion during the first $\sim 10^7$ yr (with an upper limit of 2–4 $\times$ 10^7 yr) of the population's lifetime.

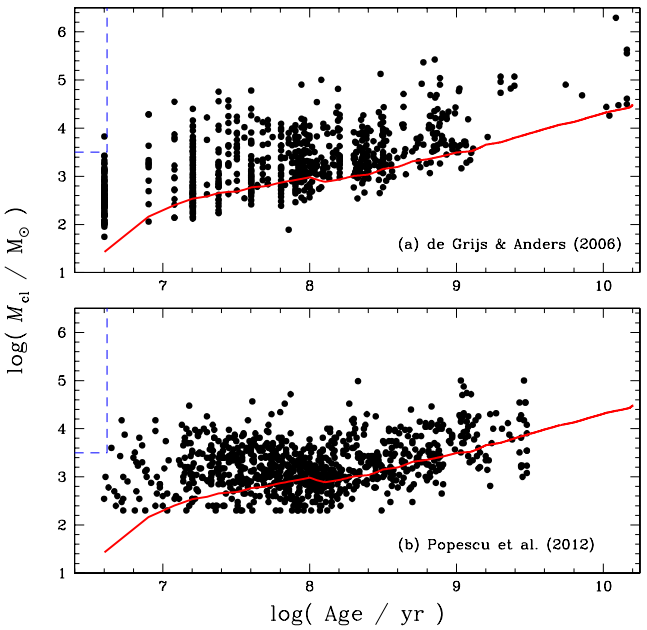

Figure 1. (a) Age–mass distribution (de Grijs & Anders 2006) of the 748 optically selected LMC clusters based on our updated data base. (b) As panel (a), but for the parameters determined by Popescu et al. (2012, their tables 1 and 2) for 920 LMC clusters. For reasons of presentational clarity, we have omitted the relevant error bars on the data points in both panels, although they have been taken into account properly in our analysis (see the text). The solid (red) lines indicate the approximate 50 per cent completeness limits, $M_V \simeq -4.3$ mag, based on the GALEV SSP models. The blue dashed boxes indicate a section of parameter space which will be discussed in Section 5.1.

Zaritsky et al. 2004) to construct colour–magnitude diagrams (CMDs) and subsequently determined ages for their entire sample based on isochrone fits. Unfortunately, the lower age boundary pertaining to the Glatt et al. (2010) sample is poorly defined. They only performed isochrone fitting of CMDs associated with objects identified as genuine clusters (flagged 'C') by Bica et al. (1996). This selection resulted in poorly understood systematic effects; however: (i) Bica et al.'s (1996) classification is, essentially, based on visual examination and hence affected by subjectivity, and (ii) very young objects are usually classified as 'associations' or 'nebulae', which leads to a subjective, *variable* lower age limit of ∼10 Myr to the Glatt et al. (2010) sample. These considerations render the applicability of the latter catalogue rather limited in the context of our assessment of the reality of early star cluster disruption in the LMC. Nevertheless, this data base can and will be used to provide circumstantial support to our results in Section 5.

3 STOCHASTICITY IN THE CLUSTERS' STELLAR MFS

In analyses of integrated star cluster photometry, one must be careful to assess the effects of stochastic sampling of the stellar initial MF (IMF). Particularly for cluster masses $M_{\rm cl} \lesssim$ a few $\times\, 10^4\,{\rm M}_\odot$, broad-band SEDs may yield significantly different ages and – to a lesser extent – masses than the true cluster parameters (e.g. Cerviño, Luridiana & Castander 2000; Cerviño et al. 2002; Cerviño & Luridiana 2004, 2006; Barker, de Grijs & Cerviño 2008; Maíz Apellániz 2009; Fouesneau & Lançon 2010; Popescu & Hanson 2010; Silva-Villa & Larsen 2010, 2011; Fouesneau et al. 2012; Popescu et al. 2012; Anders et al. 2013). Since our cluster mass estimates go down to a few $\times\, 10^3\,{\rm M}_\odot$, one should expect that our results would also be affected by stochasticity, although we point out that in de Grijs & Anders (2006) we found excellent agreement between our age estimates based on broad-band SED analysis and those from resolved photometry or spectroscopy, provided that the effects of the age–extinction and age–metallicity degeneracies are duly taken into account.

Recently, Popescu et al. (2012) re-analysed the LMC cluster photometry of Hunter et al. (2003) using their novel MASSCLEAN *age* approach, which allows one to take into account the effects of stochastic sampling of the stellar MF and, hence, determine the uncertainties associated with adoption of such MFs. The age–mass diagram based on their modelling is shown in Fig. 1(b). Although both panels of Fig. 1 show appreciable differences in the details, the overall distributions appear fairly similar in terms of their coverage of the relevant parameter space, particularly once one considers the clusters well above the 50 per cent completeness limit (e.g. both catalogues are roughly equally split into clusters younger and older than 100 Myr). Most importantly in the context of the present work, the Popescu et al. (2012) results yield significantly lower masses for a fraction of the LMC clusters (i.e. those located below the generic 50 per cent completeness limit), which is an expected effect of fitting integrated magnitudes affected by stochastically sampled stellar MFs with fully sampled SEDs (e.g. Silva-Villa & Larsen 2010, 2011; Anders et al. 2013). We also note that Popescu et al.'s (2012) cluster ages extend up to $\log(t\,{\rm yr}^{-1}) = 9.5$, while the GALEV models used to construct Fig. 1(a) include older ages. Close inspection of both sets of results shows that of the 10 clusters rendered older than $\log(t\,{\rm yr}^{-1}) = 9.5$ by our GALEV-based approach, six and four were returned as, respectively, $\log(t\,{\rm yr}^{-1}) \sim 9$ and $\log(t\,{\rm yr}^{-1}) < 8$ by the MASSCLEAN *age* approach.

Baumgardt et al. (2013, their fig. 2) compared the age determinations of de Grijs & Anders (2006) with those of Popescu et al. (2012) and found a systematic deviation from the one-to-one locus. They suggested that this tilt in the distribution is most likely

Table 1. LMC cluster positions and derived parameters.

RA (J2000)	Dec. (J2000)	M_V	$\log(t\,{\rm yr}^{-1})$			$\log(M_{\rm cl}/{\rm M}_\odot)$			Cluster name(s)
(hh mm ss.ss)	(dd mm ss.ss)	(mag)	(min)	(best)	(max)	(min)	(best)	(max)	
04 44 47.00	−69 38 31.83	−4.120	8.134	8.318	8.358	3.009	3.161	3.190	LW46, KMHK63
04 44 59.63	−70 18 05.40	−3.807	7.944	8.000	8.301	2.730	2.764	2.998	BSDL14
04 45 05.91	−68 47 43.18	−1.641	6.903	7.857	8.301	1.029	1.892	2.220	SL27, KMHK64
04 45 08.87	−69 48 11.20	−2.624	7.964	8.326	8.422	2.267	2.542	2.611	LW49, KMHK67
04 45 41.00	−70 59 23.00	−3.789	8.064	8.334	8.408	2.791	3.000	3.053	SL31, LW53, KMHK75
...	...	...	...	...	...	...	...	...	

Notes. The 1σ uncertainties in the age and mass estimates are represented by the differences between the 'best' values and the minimum/ maximum allowable solutions from the analysis of de Grijs & Anders (2006), who adopted $Z = 0.4\,{\rm Z}_\odot$ and $E(B-V) = 0.1$ mag. Table 1 is published in its entirety in the electronic edition of the paper. A portion is shown here for guidance regarding its form and content.

Table 2. Quantitative, statistical comparison of the derived LMC cluster ages for different sample selections.

Sample	Reference[a]	Slope[b]	Reference[a]	Slope[b]
All clusters	N/A	0.82 ± 0.02	N/A	0.82 ± 0.02
$\log(M_{\rm cl}/{\rm M}_\odot) \geq 3.0$	de Grijs & Anders (2006)	0.96 ± 0.04	Popescu et al. (2012)	0.90 ± 0.03
$\log(M_{\rm cl}/{\rm M}_\odot) \geq 3.5$	de Grijs & Anders (2006)	1.03 ± 0.06	Popescu et al. (2012)	1.03 ± 0.03
$\log(M_{\rm cl}/{\rm M}_\odot) \geq 4.0$	de Grijs & Anders (2006)	1.00 ± 0.11	Popescu et al. (2012)	1.07 ± 0.04

[a]Data base used to determine the lower mass limit.
[b]Horizontal axis: age determinations from de Grijs & Anders (2006); vertical axis: age determinations from Popescu et al. (2012).

caused by the effects of stochasticity. Here, we make an effort at quantifying the impact of stochastic effects, since this will be important for the discussion in the remainder of the paper. In Table 2, we compare the slope (including the statistical uncertainty in the fit) in the $\log(t\,{\rm yr}^{-1})$ (de Grijs & Anders 2006) versus $\log(t\,{\rm yr}^{-1})$ (Popescu et al. 2012) diagram for (i) different low-mass limits and (ii) using both the de Grijs & Anders (2006) and the Popescu et al. (2012) cluster mass determinations as our basis. It appears that for cluster masses $\log(M_{\rm cl}/{\rm M}_\odot) \gtrsim 3.0$–3.5 (where the value of the lower limit depends on the data base used for the mass determination), the age comparison is statistically consistent with a one-to-one distribution. Among the clusters younger than 10^9 yr (the age range of interest in this paper) in the de Grijs & Anders (2006) sample, 142 of 550 (25.8 per cent) are less massive than $\log(M_{\rm cl}/{\rm M}_\odot) = 3.0$ yet brighter than the canonical selection limit at $M_V = -4.3$ mag. A similar fraction, 21.6 per cent (119 of 552 clusters), meet the same selection criteria in the Popescu et al. (2012) sample.

This conclusion is also consistent with the statistical differences between the cluster mass determinations. Fig. 2 shows the extent to which the de Grijs & Anders (2006) and Popescu et al. (2012) masses are comparable. The top panel shows the individual mass measurements and their associated uncertainties. The bottom panel is based on the same data set, but here we use a density distribution to highlight the locus of the majority of our sample clusters. It is clear that, for clusters with $\log(M_{\rm cl}/{\rm M}_\odot) \lesssim 3.5$, the Popescu et al. (2012) masses are systematically higher than their counterparts from de Grijs & Anders (2006). For higher mass clusters, the similarity between both studies is, in fact, quite close. The masses and ages in both data sets are statistically similarly distributed for clusters with $\log(M_{\rm cl}/{\rm M}_\odot) \geq 3.5$, within the associated uncertainties. For instance, for $\log(M_{\rm cl}/{\rm M}_\odot) \geq 3.0$ (3.5), the slope in Fig. 2 is 1.04 ± 0.05 (1.00 ± 0.08).

As a result of these considerations, we are confident that the effects of stochasticity in the clusters' stellar MFs, while clearly present, do not significantly impede our analysis. In the remainder of this paper and where relevant, we will split up our sample of LMC clusters into different mass-limited subsamples, to explore specifically whether stochastic sampling effects could have a significant impact on our conclusions. Finally, and perhaps most importantly, we also note that the comparison studies using the same data base (in particular Chandar et al. 2010a,b) are similarly affected by these effects. The effects of taking into account stochastic sampling become clear when we consider the numbers of young, $\leq 10^9$-yr-old clusters between $\log(M_{\rm cl}/{\rm M}_\odot) = 3.0$ and 3.5 in both of our catalogues. We find a total of 179 clusters (32.5 per cent) of clusters in this selection box in the de Grijs & Anders (2006) data base, compared with 262 objects (47.6 per cent) in the Popescu et al. (2012) tables.

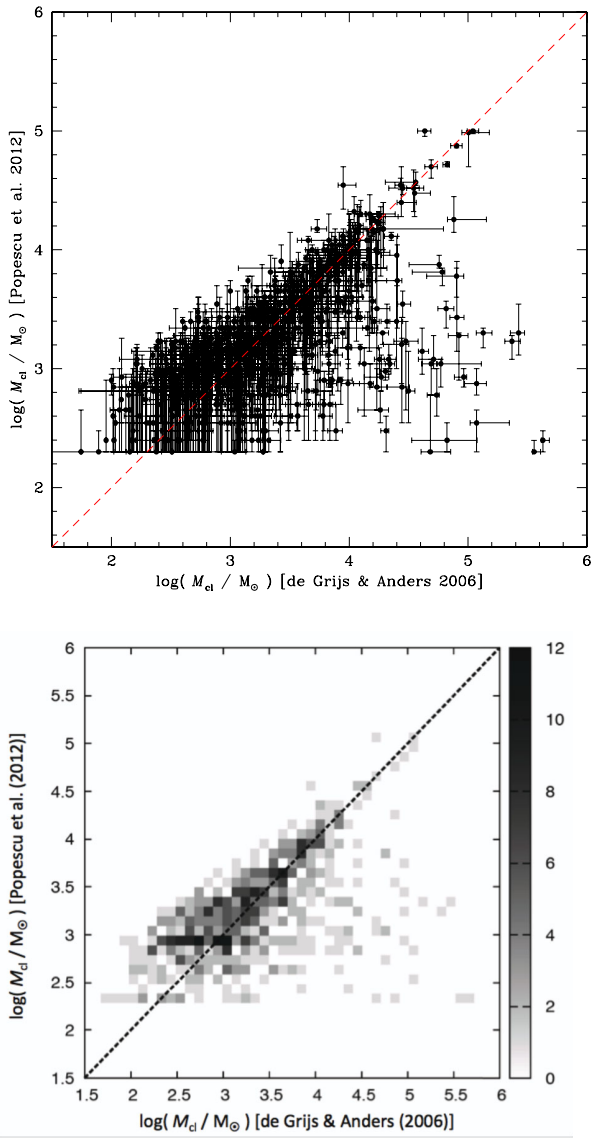

Figure 2. Comparison of cluster masses determined by de Grijs & Anders (2006) and Popescu et al. (2012). Top: direct comparison, including uncertainties. Bottom: representation as a density distribution.

4 CLUSTER MFS

In de Grijs & Goodwin (2008), we explored the potential effects of star cluster infant mortality in the SMC by analysing the cluster MFs as a function of age. Particularly for the youngest ages, cluster MFs are well described by power-law distributions of the form

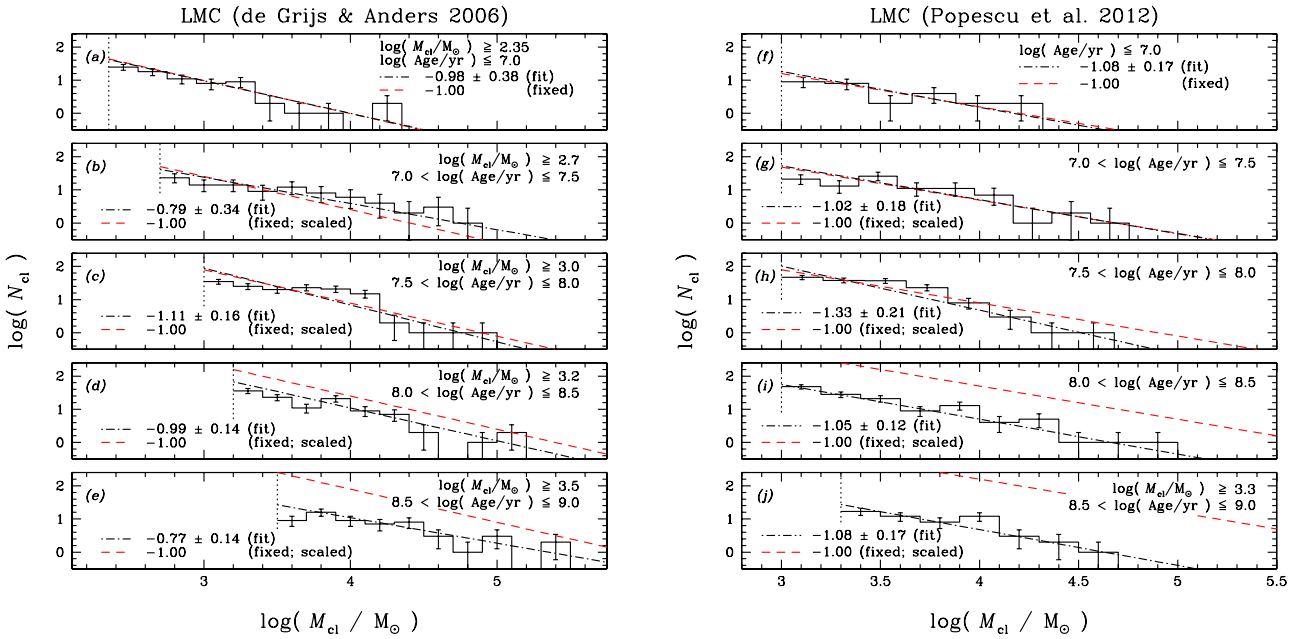

Figure 3. Cluster MFs for statistically complete LMC cluster subsamples. Age and mass ranges are indicated in most panel legends; for panels (f)–(i) we have adopted a minimum cluster mass of 10^3 M$_\odot$. The vertical dotted lines indicate the low-mass limits adopted for the power-law distributions; for panels (a)–(e) and (i)–(j), these represent the approximate 50 per cent completeness limits. The error bars represent Poissonian errors, while the (red) dashed lines represent cluster MFs of 'canonical' slope $\alpha = 2$, shifted vertically as described in the text. Except for the dashed line in the top panels, these canonical MFs are *not* fit results. The (black) dash–dotted lines represent the best-fitting cluster MFs for $3.0 \leq \log(M_{\rm cl}/{\rm M}_\odot) \leq 5.0$; for panels (d), (e) and (j) we used the selection limit as lower fitting boundary.

$N_{\rm cl} \propto M_{\rm cl}^{-\alpha}$, where $N_{\rm cl}$ is the number of clusters of mass $M_{\rm cl}$, while the power-law slope α is usually close to 2 (e.g. de Grijs et al. 2003; Portegies Zwart, McMillan & Gieles 2010; Fall & Chandar 2012). Here we apply the same analysis techniques to our LMC sample. One significant advantage of using the LMC cluster sample compared with the SMC cluster population is its approximately three-fold larger number of clusters, resulting in comparatively smaller statistical uncertainties.

Fig. 3 shows the cluster MFs for five statistically complete LMC cluster subsamples, based on both the de Grijs & Anders (2006) and Popescu et al. (2012) age and mass determinations (left- and right-hand columns, respectively). We have included the best power-law fits as black dash–dotted lines. Note that in the representation where we show $\log(N_{\rm cl})$ as a function of $\log(M_{\rm cl})$, the canonical power-law index of -2 translates into a slope of -1. It is clear that for $\log(t\,{\rm yr}^{-1}) \lesssim 8.0$–8.5 (depending on the parameter set used for the analysis), the MFs are well described by such a canonical power-law function. The red dashed lines represent these power laws with a slope of -1 in the parameter space defined by Fig. 3. In panels (b)–(e) and (g)–(j) we show the canonical MFs, scaled from the best-fitting loci in Figs 3(a) and (f), respectively, by the difference in age range between the panels. In de Grijs & Goodwin (2008), we explained that the main uncertainties introduced by adopting this method are owing to fluctuations caused by small-number statistics in the youngest age range and the exact length of the youngest age range, for which we adopted a minimum age for optically visible clusters of 3 Myr. The youngest age limit is set by the time it takes for a cluster to emerge from its natal gas and dust cloud and become optically visible (cf. de Grijs & Goodwin 2008).

The scaled canonical cluster MFs provide remarkably good matches to the MFs in, respectively, panels (b), (c) and (g), (h), given the simplifying underlying (null) hypothesis of constant cluster formation. The small apparent difference between the canonical and best-fitting slopes in panel (b) – although they are still comparable within the formal statistical uncertainties – is likely owing to the appearance of red supergiants in this age range, combined with the possible effects of stochasticity. (The presence of red supergiants in stochastically sampled clusters will cause SED fits based on fully sampled IMFs to return cluster masses that are biased towards higher values.) Stochastic sampling effects are also the likely cause for the $\sim$1–2σ slope discrepancy seen in panel (h). Based on this analysis alone, it appears that the effects of significant cluster disruption become apparent only beyond $\log(t\,{\rm yr}^{-1}) \sim 8$. Although we do not claim that this result on its own validates the assumption of constant cluster formation, nor the absence of rapid cluster disruption in the LMC, it contributes to the overall, self-consistent picture of early cluster evolution which we are painting in this paper.

Under the assumption that the cluster formation rate has remained roughly constant (within 10 per cent for $t \leq 10^9$ yr; cf. Maschberger & Kroupa 2011; see also Section 6.1), we conclude on the basis of Fig. 3 that there is no compelling evidence of significant mortality, either infant mortality or disruption up to $\sim$100 Myr and within the Poissonian uncertainties. In the next section, we will attempt to quantify the maximum disruption rate allowed by the data and the corresponding uncertainties.

5 DISRUPTION OR EVOLUTION?

To underscore the key result from the previous section, in Fig. 4 we plot the LMC cluster age distribution expressed in number of clusters per Myr. We show both the full magnitude-limited LMC cluster sample and three mass-limited subsamples. In addition, we have included two arrows to highlight the main differences between

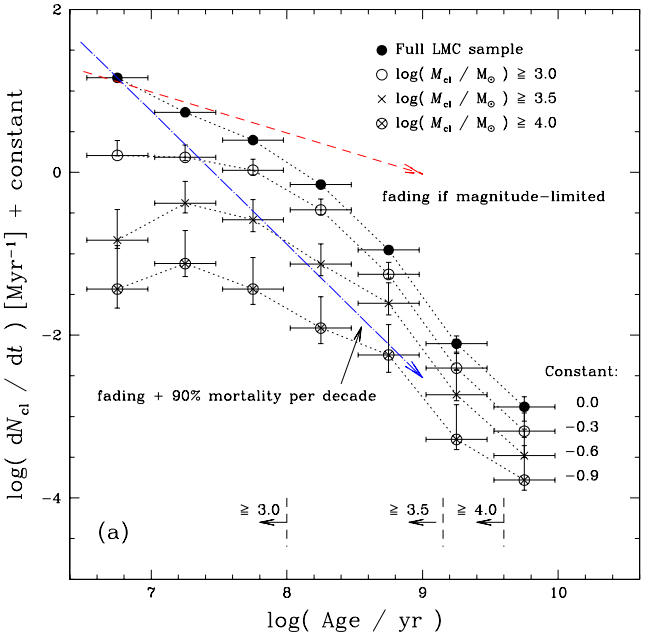

Figure 4. LMC cluster age distribution expressed as number of clusters per Myr. Shown are four different samples, including the full magnitude-limited LMC sample and three mass-limited subsamples (shifted vertically, for reasons of clarity, by the constant offsets indicated). The mass-limited subsamples are 50 per cent complete to the left of the vertical dashed lines included at the bottom of the figure, where the numbers refer to the 50 per cent completeness limits for a given range, expressed in log ($M_{cl}/M_\odot$). The vertical error bars are Poissonian errors; the horizontal error bars indicate the age ranges used for the generation of these data points. The dashed arrow shows the expected effects due to evolutionary fading of a cluster sample made up of SSPs, based on the GALEV SSP models, while the dash–dotted arrow represents the combined effects of a fading cluster population and 90 per cent cluster disruption per decade in log (t yr^{-1}).

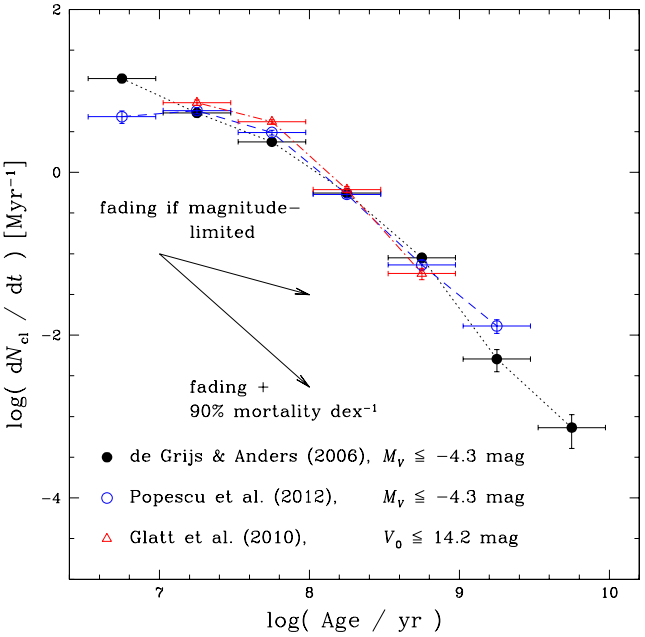

Figure 5. As Fig. 4, but for magnitude-limited subsamples based on all three catalogues discussed in this paper.

the theoretical expectations for no cluster infant mortality and a 90 per cent disruption rate per decade in age. Both predictions also include the usual effects of stellar evolution and fading, i.e. they follow standard SSP evolution as implemented in the GALEV models. Just as for the SMC cluster system, if we force it to pass through the data point associated with the youngest age range, the blue long-dashed arrow does not appear to describe *any* of the trends even remotely satisfactorily for ages up to $t = 10^8$ yr. Specifically, we can rule out a 90 per cent disruption rate per decade of age up to an age of 1 Gyr at the $\gtrsim 8\sigma$ level (where σ refers to the Poissonian uncertainties shown in Fig. 4).

As additional support of this conclusion, in Fig. 5 we reproduce the LMC cluster age distribution based on the full de Grijs & Anders (2006) sample (Fig. 4), and add the equivalent distributions based on both the Popescu et al. (2012) and the Glatt et al. (2010) catalogues, using the same selection limit. Although the Glatt et al. (2010) data base includes stars down to $V \sim 24$ mag, their LMC stellar census used to construct cluster CMDs is significantly incomplete below $V \simeq 23$ mag (which limits their cluster age determinations to a maximum of ∼1 Gyr). This implies that many low-mass, low-luminosity clusters are likely yet to be detected. The census of brighter, more massive clusters is significantly more complete and comparable among all studies (cf. Baumgardt et al. 2013). However, since in this paper we will apply the same selection limits to the Glatt et al. (2010) data as to the de Grijs & Anders (2006) and Popescu et al. (2012) samples,[2] the results should be comparable for the appropriate age ranges. Recall that Glatt et al. (2010) only considered clusters aged between ∼10 Myr and 1 Gyr, but note as a caveat that for the youngest ages in the catalogue the cluster census may be somewhat incomplete owing to a potentially variable lower age limit (see Section 2). These authors provide ages, extinction values and integrated V-band photometry for all clusters in their sample; although they do not state specifically whether their V-band magnitudes have been extinction corrected, our interpretation of their description is that they are (but this makes a negligible difference to our results, in any case).

Reassuringly, all three distributions exhibit the same overall behaviour and even their absolute scaling renders the distributions virtually indistinguishable. All three samples, based on two independent photometric catalogues and three independently determined age distributions, are consistent with an age distribution for ages up to $\sim 10^8$ yr that is best described by simple stellar evolution (i.e. evolutionary fading), without the need for additional disruption. In all three cases, the slope of the distribution becomes significantly steeper only for ages in excess of 100 Myr, where we are likely witnessing the onset of dynamical disruption (cf. Boutloukos & Lamers 2003; Lamers et al. 2005).

If we now compare Figs 4 and 5 with fig. 17 (left) of Chandar et al. (2010a), we first note that for ages $\gtrsim 10^8$ yr, the overall distributions appear fairly similar, with a significant steepening of the distribution occurring around 100 Myr. However, for younger ages, the Chandar et al. (2010a) distribution is 'negatively curved', compared with the 'positively curved' age distributions resulting from the three catalogues considered in this paper. In fact, this appearance is predominantly driven by Chandar et al.'s (2010a) youngest age bin, which exhibits a clear excess in cluster numbers compared with the youngest age bin in the other distributions discussed in this

[2] To convert the apparent magnitudes of Glatt et al. (2010) to absolute magnitudes, we adopted the canonical LMC distance modulus of $(m - M)_0 = 18.50$ mag.

context. We will explore the background to this apparent discrepancy in the next section.

5.1 Discrepancies

Note that one of the main differences between our results and those of Chandar et al. (2010a,b) is driven by our respective analysis methods. Chandar et al. (2010a,b) characterize their entire age- and mass-limited cluster (sub)samples by a single disruption law (i.e. a straight-line fit in their equivalent representations of our Fig. 4), which may not be warranted, as we show here. Our approach, on the other hand, is to explore whether a 90 per cent disruption rate is supported for the earliest age ranges. The differences between both sets of results therefore hinge on the treatment of the data points pertaining to the youngest ages.

We will, therefore, perform a detailed comparison of Chandar et al.'s (2010a) age–mass diagram (their fig. 3; top panel) with the equivalent diagrams shown in Fig. 1. The main differences in the cluster distributions between de Grijs & Anders (2006) and Chandar et al. (2010a) are (i) the presence of a population of young, high-mass clusters in the Chandar et al. (2010a) data set, which are virtually absent in the de Grijs & Anders (2006) results, and (ii) an overdensity (chimney) of clusters near $\log(t\,\mathrm{yr}^{-1}) \simeq 6.6$ in the Chandar et al. (2010a) data. The latter overdensity is related to the fitting procedure, as already acknowledged by Chandar et al. (2010a) in the context of their comparison with the original Hunter et al. (2003) results. Similar overdensities, although for different ages, are seen in our age–mass diagram of Fig. 1(a) (cf. Section 2). This type of behaviour is inherent to the use of broad-band SEDs to determine integrated cluster properties.

The significant difference in the number of young, high-mass clusters between both studies is more worrying: such objects are among the brightest sources in a given cluster sample and should therefore be found in any analysis. To explore the reason for this discrepancy, we specifically focus on the section of parameter space covered by $\log(t\,\mathrm{yr}^{-1}) \leq 6.6$ and $\log(M_{\rm cl}/\mathrm{M}_\odot) \geq 3.5$, indicated by the blue dashed boxes in Figs 1(a) and (b). Since the parameters derived by Chandar et al. (2010a) are not publicly available, we base our comparison on their published figure. In the relevant section of parameter space, Chandar et al. (2010a) include 18 objects in their fig. 3 (top panel). The equivalent region contains a single source in de Grijs & Anders (2006), whereas in Popescu et al. (2012) this region remains unoccupied. We re-emphasize that all of these studies used the same photometric data base as input for their cluster age and mass distributions.

Chandar et al. (2010a) based their broad-band SED fits on the Bruzual & Charlot (2003) SSPs for $Z = 0.008$, a Salpeter (1955)-type IMF and Fitzpatrick's (1999) Galactic extinction law. Although de Grijs & Anders (2006) and Popescu et al. (2012) used different SSP models and extinction laws, these choices are not expected to lead to significantly different cluster age and mass estimates (cf. de Grijs et al. 2005). The main difference between the approach taken by Chandar et al. (2010a) on the one hand and that taken by de Grijs & Anders (2006) and Popescu et al. (2012) on the other resides in the choice of stellar IMF. The latter studies used a Kroupa (2002)-type IMF, which would yield lower cluster masses by a factor of $\sim$3.8 (or $\sim$0.6 dex) compared to the use of a Salpeter (1955) IMF. However, Chandar et al. (2010a) argue that this difference is offset by the need to apply aperture corrections to the original integrated cluster photometry, thus eventually leading to similar masses. Finally, we note that the youngest isochrone in the GALEV SSP models is characterized by an age of $\log(t\,\mathrm{yr}^{-1}) = 6.6$, whereas the youngest object in Chandar et al. (2010a) in the parameter space of interest has an age of $\log(t\,\mathrm{yr}^{-1}) \simeq 6.26$ (1.8 Myr); we considered this too young for a cluster to have emerged from its natal molecular and dust cloud (cf. Section 4).

With these differences in mind, we reverse engineered the photometric measurements in the Johnson V band (with and without extinction corrections) that would be associated with the Chandar et al. (2010a) age/mass combinations for the youngest, highest mass clusters located in the dashed regions in Fig. 1. On the basis of a comparison of the V-band magnitudes thus derived with the original integrated cluster photometry, we conclude the following:

(i) the majority of the objects in this region with cluster parameters derived by Chandar et al. (2010a) are up to 3 mag brighter than any of the clusters in the original photometric data base; and

(ii) a handful of the youngest, lowest mass clusters (parameters as derived by Chandar et al. 2010a) may have counterparts in the de Grijs & Anders (2006) and Popescu et al. (2012) data sets, although in these instances the latter authors obtained best-fitting parameters corresponding to older, more massive clusters. Such discrepancies can be traced back to the well-known age–extinction(–metallicity) degeneracy and are not a real reason for serious concerns in the context of this paper.

Thus, while some of the lower mass clusters of Chandar et al. (2010a) in the section of parameter space of interest could have counterparts in our own and the Popescu et al. (2012) data bases, we are unable to identify the highest mass clusters in Chandar et al. (2010a) in the original data set that forms the basis for all three analyses. Yet, it is this subsample of clusters that drives the controversy and the conclusion that significant cluster disruption may affect the LMC cluster sample from the youngest ages onwards. Based on the comparison performed here, we are forced to conclude that, in retrospect, this claim appears to be unwarranted. In the following, we will attempt to place this conclusion on a firmer quantitative footing.

5.2 Cumulative distribution functions

For any of the mass-limited subsamples, significant disruption does not occur until $t \gtrsim 10^8$ yr (cf. Parmentier & de Grijs 2008; Baumgardt et al. 2013); for the full LMC cluster sample, one could argue that some effects of disruption, in addition to evolutionary fading, start to appear for $\log(t\,\mathrm{yr}^{-1}) \gtrsim 7.5$. Note that this age range is beyond that where we would consider the relevant disruption process 'infant' mortality (although this is a matter of semantics).

Using a Monte Carlo approach, we will now attempt to quantify the rate of disruption allowed by the data, using the cumulative cluster age distribution. Our basic assumption is that clusters are born uniformly in (linear) time following a power-law MF, $N(M_0) \propto M_0^{-\alpha}$, where $\alpha = 2$. Irrespective of the effects of infant mortality, if any, clusters evolve owing to stellar evolution and two-body relaxation according to the formalism of Lamers et al. (2005). The fraction of the mass of a cluster with initial mass M_0 that is still bound at age t is given by

$$\mu_{\rm ev}(t) \equiv \frac{M_{\rm cl}(t)}{M_0} = 1 - q_{\rm ev}(t), \tag{1}$$

where $q_{\rm ev}$ is the mass lost through stellar evolution,

$$\log q_{\rm ev} = (\log t - a_{\rm ev})^{b_{\rm ev}} + c_{\rm ev}, \tag{2}$$

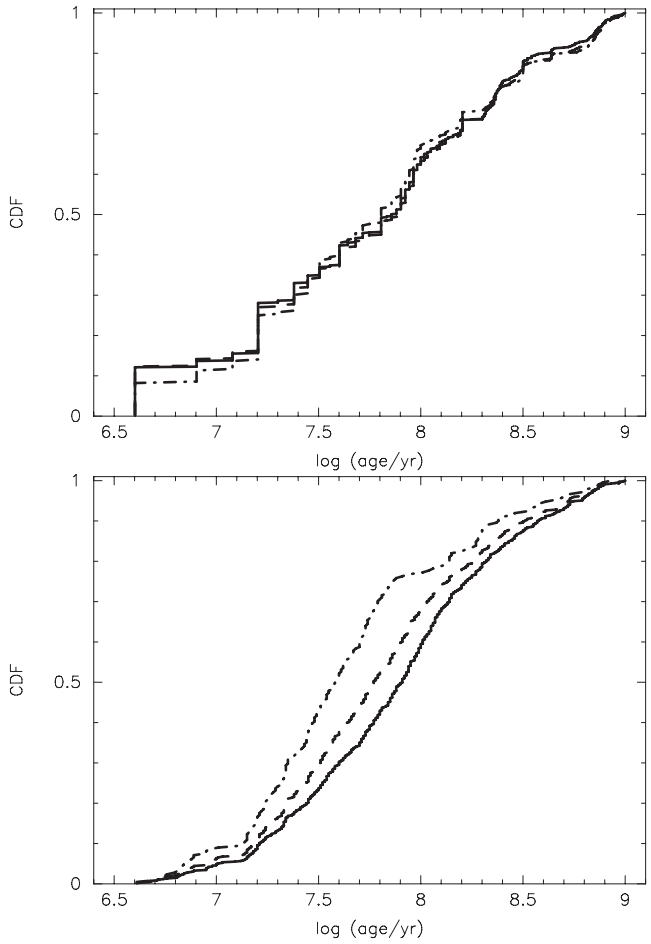

Figure 6. Top: cumulative distribution functions (CDFs) based on the de Grijs & Anders (2006) cluster sample for 'selection factors' $S = 0$, 0.5 and 1 – as defined in equation (4) – represented by the solid, dashed and dash–dotted lines, respectively. Bottom: as the top panel, but for the Popescu et al. (2012) sample.

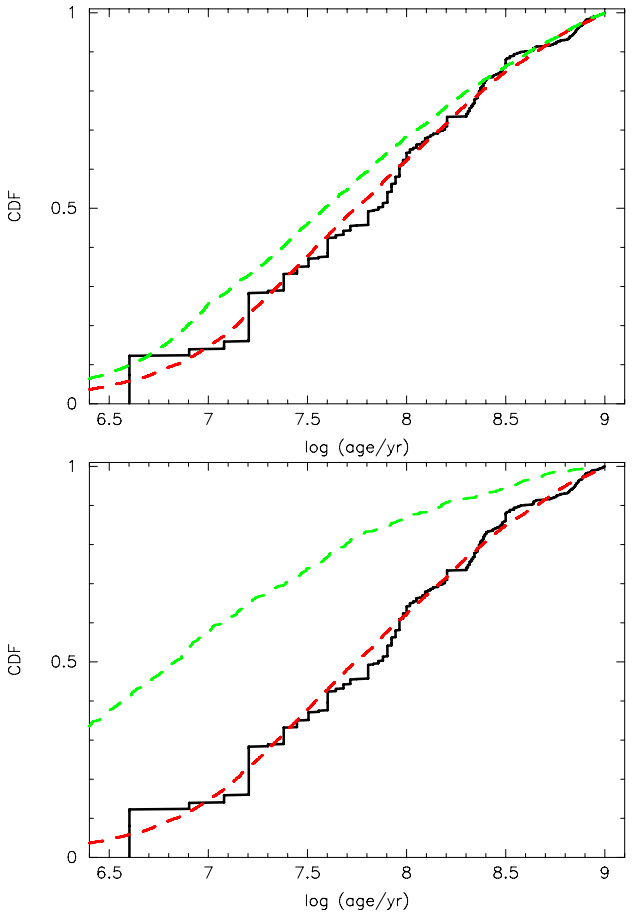

Figure 7. CDFs of the LMC cluster age distribution. The solid lines represent the de Grijs & Anders (2006) data for $S = 0$; the red dashed lines denote the best fit for $t > 4 \times 10^6$ yr (our lower boundary), assuming no disruption (specifically, no infant mortality), again for $S = 0$. Green dashed lines: predicted CDFs for 50 per cent infant mortality at an age of 10 Myr, followed by stellar evolutionary and dynamical evolution from the models of Lamers et al. (2005), adopting $t_0 = 10^6$ yr (top), and 90 per cent mortality per decade in $\log(t\,\mathrm{yr}^{-1})$ and minimal evolution, i.e. $t_0 = 10^9$ yr (bottom), for $t \leq 10^9$ yr, normalized at $t = 10^9$ yr.

and $a_{\rm ev} = 7$, $b_{\rm ev} = 0.255$ and $c_{\rm ev} = -1.820$. The 'tidal' parameter t_0, defined as the normalization factor of the disruption time-scale,

$$t_{\rm dis} = t_0 \left(\frac{M_{\rm cl}}{\mathrm{M}_\odot} \right)^{\gamma} \qquad (3)$$

(and $\gamma = 0.67$ in our model; cf. Boutloukos & Lamers 2003), can be varied, but it only makes a measurable difference to our results if $t_0 < 10^6$ yr, which has been ruled out by a prior analysis of the LMC cluster sample, which also established that $t_{\rm dis,\,LMC} > 10^9$ yr for 10^4 $\mathrm{M}_\odot$ clusters (Parmentier & de Grijs 2008). Therefore, the cluster mass at age t will simply be a function of M_0 and age, modulo the t_0 parameter.

Clusters are observed if their mass at a particular age is higher than some limiting mass, $M_{\rm lim}(t)$ (defined by the observational completeness limit), which is well represented by

$$\log(M_{\rm lim}/\mathrm{M}_\odot) = 0.5 \log(t\ \mathrm{yr}^{-1}) - 1.5 + S, \qquad (4)$$

where S is a 'selection factor' which allows us to explore the importance of varying the selection limit: $S = 0$ roughly follows the selection limit of the observations for $6.5 < \log(t\,\mathrm{yr}^{-1}) < 9$ (see Fig. 1), while for $S = 0.5$ this limit moves up by $\Delta\log(M_{\rm cl}/\mathrm{M}_\odot) = 0.5$.

Fig. 6 shows the LMC clusters' cumulative distribution functions (CDFs) for (top) the de Grijs & Anders (2006) catalogue and (bottom) the Popescu et al. (2012) data base using $S = 0$, 0.5 and 1 as selection limits. In the top panel, the CDFs contain, respectively, 709, 544 and 256 clusters; the equivalent numbers in the bottom panel are 671, 473 and 211 clusters, respectively. Interestingly, the de Grijs & Anders (2006) CDFs for different values of S are essentially the same [we will discuss the differences seen in the Popescu et al. (2012) data below]. There is no apparent correlation between the numbers of clusters in any age range with cluster mass (although the total numbers change), which is consistent with a roughly constant cluster formation rate. In addition, if any significant level of cluster disruption were at play, the data are also consistent with no strong mass dependence.

Fig. 7 shows the CDF of the LMC cluster population based on the de Grijs & Anders (2006) sample (solid line, where the sudden jumps are caused by the chimneys in the data set). The red dashed lines represent the CDF (for $S = 0$) of the artificially generated Monte Carlo clusters characterized by a constant cluster formation rate and based on standard N-body dynamics, including the effects of stellar evolution but no infant mortality. Note that in all cases where we show CDFs, here and below, the data and model must necessarily match at a cumulative fraction of unity, which

represents our normalization. The observations are well fitted by a model without the need for any significantly enhanced (infant) mortality after 4 Myr, beyond the disruption that would be expected from the combined action of stellar evolution and stellar dynamics (predominantly two-body relaxation) on time-scales up to 10^9 yr. Note that we model such evolution using the analytic prescription of Lamers et al. (2005). In reality, the t_0 parameter would vary with position and time, which may lead to some (possibly significant) differences to the cluster disruption properties and time-scales at different galactocentric radii (see, e.g., Bastian et al. 2012). A small amount of additional disruption (either infant mortality or dynamical dissolution) could be accommodated by the data, but there is no need to do so. Where our models include the effects of infant mortality, this is implemented by the removal of a given fraction (as specified in the text) of the star cluster population at an age of 10 Myr, irrespective of cluster mass.

The top panel of Fig. 7 also shows the expected CDF for 50 per cent cluster infant mortality at an age of 10 Myr, followed by standard stellar and dynamical evolution, for the same t_0. Although t_0 is a free parameter, the observational data are inconsistent with significant early disruption, irrespective of the value of t_0: in essence, early (infant) mortality causes a change in the CDF slope at early times, which remains. The smooth shape of the data suggests no 'kink' and, therefore, no significant infant mortality.

The bottom panel of Fig. 7 explores the idea of a 90 per cent disruption rate per decade in $\log(t\,\mathrm{yr}^{-1})$ up to $t = 10^9$ yr. The green dashed line is the closest that this model (i.e. for $t_0 = 10^9$ yr) is found to approach the data, given that the data and the model must reach a cumulative fraction of unity at the same time; it is clearly a very poor match. The main problem with this model is that to find any clusters at all at the oldest ages requires very large numbers of clusters at young ages, as shown by the difference between the green dashed line and the data at the youngest ages: instead of the observed fraction of <15 per cent, more than half of our sample clusters would need to be younger than 10 Myr. If this were the case, this would suggest significant deviations from the roughly constant cluster formation rate implied by the observational data (e.g. Maschberger & Kroupa 2011; see also Section 6.1).

In the context of our comparison with the Chandar et al. (2010a,b) results, the de Grijs & Anders (2006) data base is the most appropriate comparison sample, given that it is also based on SED fits assuming fully sampled cluster stellar IMFs. This notion is supported by Chandar et al.'s (2010a,b) conclusion that the impact of sample incompleteness on their results is minimal at the low-mass end, as we also found for the de Grijs & Anders (2006) sample. The effects caused by stochastic sampling of the stellar MFs become apparent in the bottom panel of Fig. 7. Whereas the Popescu et al. (2012) data describe a qualitatively similar behaviour as those in the top panel of that figure in terms of the absence of a clear need for significant cluster disruption to have occurred in the last $\sim$100 Myr, taking into account stochastic sampling tends to lead to an overproduction of massive clusters aged between approximately 10 and 30 Myr, compared to the results from 'standard' modelling. This effect becomes apparent for $S = 1$, i.e. well above our selection limit; for $S = 0$ and 0.5, the Popescu et al. (2012) results are, in fact, similar to (although not the same as) the de Grijs & Anders (2006) CDFs.

5.3 A variable cluster formation rate?

Figs 8 and 9 illustrate and summarize the expected effects of cluster infant mortality and of changing the cluster formation rate and

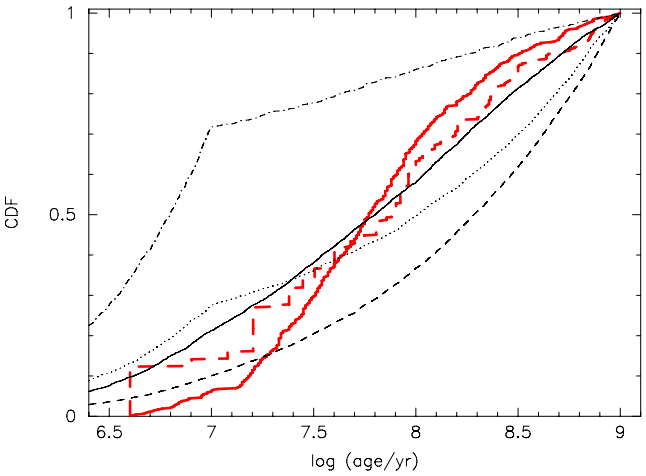

Figure 8. CDFs of the LMC cluster age distributions based on both data sets considered in this paper (for $S = 0$). The thick red lines represent the data sets (solid line: Popescu et al. 2012; dashed line: de Grijs & Anders 2006); the black lines show various model predictions. All models adopt a power-law initial cluster MF with an index of $\alpha = 2$. From top to bottom, the models include (dash–dotted line) a scenario of 90 per cent mass-independent infant mortality at 10 Myr, followed by stellar evolution and dynamical cluster disruption characterized by $t_0 = 10^6$ yr; (solid line) a scenario based on a constant cluster formation rate and dynamical cluster disruption following Lamers et al. (2005) for $t_0 = 10^6$ yr; (dashed line) the same model as represented by the solid line, but for $t_0 = 10^7$ yr; (dotted line) a model showing the predictions for 70 per cent mass-independent infant mortality at 10 Myr, followed by stellar evolution and dynamical cluster disruption characterized by $t_0 = 10^7$ yr.

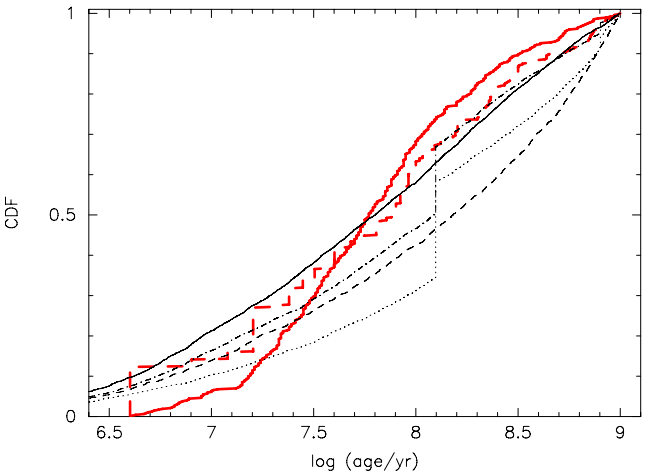

Figure 9. CDFs of the LMC cluster age distributions based on both data sets considered in this paper (again for $S = 0$), exploring the effects of varying the cluster formation rate. The thick red lines represent the data sets (solid line: Popescu et al. 2012; dashed line: de Grijs & Anders 2006); the black lines show various model predictions. All models adopt a power-law initial cluster MF with an index of $\alpha = 2$ and dynamical cluster disruption following Lamers et al. (2005) for $t_0 = 10^6$ yr. From top to bottom, the models include (solid line) the reference scenario (identical to the solid line in Fig. 8) based on a constant cluster formation rate; (dash–dotted line) a constant cluster formation rate in linear time with two additional bursts of cluster formation at 125 and 800 Myr, each of which formed 10 per cent of the total number of clusters; (dashed line) a continuously decreasing cluster formation rate (in linear time) by a factor of 4 between 1 Gyr and the present time; (dotted line) a decreasing cluster formation rate (in linear time), but with the addition of two bursts at 125 and 800 Myr. The latter model is hence a combination of the dash–dotted and dashed lines.

the characteristic disruption time-scale, t_0. Both figures show the de Grijs & Anders (2006) and Popescu et al. (2012) data sets for $S = 0$ (thick dashed and solid red lines, respectively), as well as four representative models each (black lines of different styles). All models adopt a power-law initial cluster MF with an index of $\alpha = 2$, and dynamical cluster disruption following the Lamers et al. (2005) prescription. The models in Fig. 8 are based on a constant cluster formation rate, combined with cluster disruption for $t_0 = 10^6$ and 10^7 yr (black solid and dashed lines, respectively). The black dash–dotted line represents a scenario of 90 per cent mass-independent infant mortality at 10 Myr, followed by stellar evolution and dynamical cluster disruption characterized by $t_0 = 10^6$ yr (cf. Fig. 7). Similarly, the black dotted line is for 70 per cent mass-independent infant mortality at 10 Myr and disruption characterized by $t_0 = 10^7$ yr.

A straight line in this diagram would represent equal numbers of clusters per decade in age. This is, in essence, shown by the black solid line, combined with a short characteristic disruption time-scale ($t_0 = 10^6$ yr). The black dashed line in Fig. 8 is relevant for a population containing a larger number of older clusters (closer to equal numbers per linear time period), since t_0 is longer, at 10^7 yr. If the LMC cluster population were characterized by a scenario in which 90 per cent of clusters had suffered from infant mortality (as suggested by Chandar et al. 2010a,b), the vast majority of clusters would need to be young, since only 10 per cent would survive and contribute to the observed CDF.

The alternative to the scenario represented by the black solid line (no infant mortality and a short characteristic disruption time-scale) would be evolutionary conditions dominated by $t_0 \sim 10^7$ yr and at most a small amount of infant mortality acting on time-scales up to a few $\times\ 10^7$ yr. The dotted line in Fig. 8 is based on the assumption that all infant mortality has occurred by $t = 10^7$ yr. Infant mortality which acts by an age of a few $\times\ 10^7$ yr, as usually adopted, causes a clearly discernible kink in the CDF, which in turn causes the model to attain values that are significantly too large at the youngest ages and not seen in either of our data sets. As such, neither of our data sets support a significant amount of infant mortality at early times ($t \lesssim$ a few $\times\ 10^7$ yr).

Fig. 9 shows the effect on the CDF of changing the cluster formation rate. The thin black lines show four different scenarios for the LMC's cluster formation history over the past Gyr for a characteristic dissolution time-scale $t_0 = 10^6$ yr. None of the models in this figure include any infant mortality; they only include evolutionary fading of their stellar populations and evaporation owing to dynamical evolution.

Increasing the past cluster formation rate (through adoption of either a generally higher rate or in a series of bursts) leads, unsurprisingly, to an increase in the number of clusters at older ages. The effect of introducing bursts of cluster formation are more or less obvious, depending on the fraction of the total number of clusters formed in these bursts. As an example, we adopted a scenario in which 10 per cent of the total number of clusters were formed in each instantaneous burst. Although this is admittedly excessive, it helps to illustrate the point we want to convey based on Fig. 9.

It might naïvely be thought that increasing the past cluster formation rate – and so increasing the number of older clusters relative to younger clusters – would give scope for an enhanced rate of infant mortality. However, in Fig. 9 the model CDFs for higher past cluster formation rates lie below the observations, whilst in Fig. 8 including infant mortality, combined with a constant cluster formation rate, means that there are too few old clusters compared to the observations. Let us now consider what this means for a scenario of 'classical' infant mortality. If infant mortality is rapid (i.e. caused by gas expulsion shortly after cluster formation), then the infant-mortality-induced loss of clusters from one's sample occurs after some 10–20 Myr. Therefore, it is at the very youngest ages that clusters must be vastly overproduced relative to the observations. Including a decreasing cluster formation rate with time lowers the (dash–dotted) 90 per cent infant mortality model line in Fig. 8 to some extent, but still over half of the clusters in our samples should be $<$10 Myr old compared to the 15 per cent that is observed.

In summary, the relatively small number of young clusters in both the de Grijs & Anders (2006) and the Popescu et al. (2012) samples implies that a scenario in which 90 per cent of the cluster population undergoes infant mortality is unrealistic and not supported by either data set. Alternatively, a longer characteristic disruption time-scale appears to be ruled out as well, given that there are too few old clusters in either of our catalogues to support such a model. In addition, adoption of a longer disruption time-scale will cause the CDF to be increasingly shifted to older ages, hence leading to ever more significant model *under* predictions compared with the behaviour of the actual data sets.

Finally, although we set out to show that a scenario involving 90 per cent cluster infant mortality at early times appears to be ruled out by both data sets, we will now comment briefly on the shapes of the CDFs defined by our two data sets. Although they are largely consistent with one another for $S = 0$, the data sets exhibit some small systematic differences, in particular for the youngest clusters ($t \lesssim$ a few $\times\ 10^7$ yr). In the context of the diagnostic age–mass diagram, we attributed this to the effects of stochastic sampling of the clusters' stellar MFs. In relation to the CDFs discussed in this section, these differences may be either realistic or caused by a preferential reduction of cluster masses based on stochastic modelling. We are, indeed, concerned that such a bias may have been introduced by the stochastic modelling approach. We are currently exploring these issues using our newly developed, extensive stochastic model set based on the GALEV stellar population models (Anders et al. 2013). We will apply these models to our unprecedented *Hubble Space Telescope*-based imaging data set of the rich star cluster system associated with the dwarf starburst galaxy NGC 5253 (de Grijs et al. 2013), which covers 10 passbands from near-ultraviolet to near-infrared wavelengths.

If, on the other hand, these systematic differences reflect the true physical properties of the LMC cluster sample as derived by Popescu et al. (2012), what would this mean for our analysis in this section? The de Grijs & Anders (2006) data set appears to be well represented by a roughly constant cluster formation rate over the time span considered here; to match the Popescu et al. (2012) data set, a scenario involving a slight enhancement or a minor burst in the cluster formation rate in the past few $\times\ 10^7$ yr might provide a somewhat better match. One can, of course, vary past cluster formation rates and different prescriptions of cluster mortality (infant or otherwise) to find a good fit to the observations. For example, a generally decreasing cluster formation rate but with periods of enhanced cluster formation in the past 100 Myr provides a good fit without the need to invoke infant mortality. Vastly increased cluster formation 50–300 Myr ago with significant infant mortality can also produce a reasonable fit (even though such a scenario predicts almost no 20–50-Myr-old clusters). An acceptable fit can also be obtained with significant cluster mortality occurring at 100 Myr rather than 10 Myr. However, without a good physical reason to think that these are reasonable models, particularly in the absence of supporting evidence for such scenarios based on independent

studies (see also Section 6.1), we argue that it is rather pointless to pursue such fits.

6 CONTEXT

We have thus far specifically focused on a detailed and thorough (re-)analysis of the LMC cluster population as covered by the Hunter et al. (2003) data base. Since a number of different authors reached conflicting conclusions as regards the early evolution of the galaxy's cluster system, but based on the same basic photometric data set, our aim was to explore the underlying reasons for this discrepancy. In this section, we take the discussion further by addressing the more general context associated with this work. In particular, we will address (i) the key assumption that the LMC's cluster formation history has remained roughly constant over the past $\sim$1 Gyr, and (ii) the impact of the partial coverage of the LMC's extent by the Hunter et al. (2003) cluster data base on our understanding of the LMC cluster population's properties and evolutionary history as a whole.

6.1 The LMC's cluster formation rate

Under the key assumption that the cluster formation rate has remained roughly constant, our 'null hypothesis', we concluded that there is no compelling evidence (within the uncertainties) of significant cluster disruption for $t \lesssim 100$ Myr. Our analysis of the shape and normalization of the cluster MFs, aided by our results from an assessment of the CDFs for different selection limits, supports the notion of a roughly constant cluster formation rate. In this section, we will address the validity of this assumption, so as to place our results in the more general context of the LMC's overall star and cluster formation history.

Prior to the series of papers based on the Hunter et al. (2003) photometric cluster data base, the only 'modern' analyses of the LMC's cluster formation history were published by Girardi et al. (1995) and Pietrzyński & Udalski (2000). Girardi et al. (1995) analysed integrated *UBV* photometry from a pre-publication release of Bica et al.'s (1996) catalogue and concluded that the LMC's evolutionary history is characterized by periods of enhanced cluster formation, by a factor of $\lesssim$2, at $\sim$100 Myr and 1–2 Gyr, as well as by the well-known, pronounced 'age gap' between $\sim$3 and 12–15 Gyr (see below). Pietrzyński & Udalski (2000) used ischrone fits to determine ages of up to 1.2 Gyr of 600 clusters in the central LMC (bar) area. They concluded that the LMC cluster formation rate is characterized by a number of bursts with complex age structure, specifically centred at ages of $\sim$7, 125 and 800 Myr. The most recent period of enhanced cluster formation produced a factor of 1.5–2 more clusters per unit (linear) age range than the equivalent rate during the galaxy's more quiescent period(s), while the burst centred at $\sim$125 Myr produced cluster numbers boosted by yet another factor of $\sim$2 – when we smooth the Pietrzyński & Udalski (2000) cluster age distribution to the same resolution as adopted in this paper.

However, the empirically derived cluster age distribution is the product of cluster formation *and* disruption as a function of time. Adopting the cluster age distribution as proxy of a galaxy's cluster *formation* history only yields, therefore, merely part of the story. A roughly constant age distribution could therefore imply a similarly shaped cluster formation history, but it could also result from a balanced interplay between cluster formation and disruption.

A number of authors have suggested that the LMC's resolved stellar population could provide clues as to the galaxy's cluster formation history based on CMD analysis (for a recent discussion, see Maschberger & Kroupa 2011), provided that the star and cluster formation histories can be mapped on to one another within reasonably small uncertainties. However, (massive) cluster and field-star formation may well require different conditions to thrive in, implying that the two formation scenarios may not always be coincident. This type of scenario is likely, in fact, given the observed disparities between the cluster and field-star age distributions in, e.g., the Magellanic Clouds as well as in NGC 1569 (e.g. Anders et al. 2004a). In particular, the LMC exhibits a well-known gap in the cluster age distribution, although the age distribution of the field stellar population appears more continuous (e.g. Olszewski, Suntzeff & Mateo 1996; Geha et al. 1998; Sarajedini 1998, and references therein). In addition, the cluster and field-star age distributions are also significantly different in the SMC (cf. Rafelski & Zaritsky 2005; Gieles et al. 2007).

Maschberger & Kroupa (2011) recently performed a very careful and detailed study of the LMC's cluster formation history (based on the ages and masses from de Grijs & Anders 2006) and its relationship, if any, with the galaxy's field-star formation history. They compared the LMC's star formation history based on CMD analysis (using observational data from Harris & Zaritsky 2009) with the galaxy's cluster formation history resulting from consideration of both the most massive clusters only (cf. Maschberger & Kroupa 2007) and of the total mass in clusters of any mass, although in the latter case they could trace only the most recent 20–400] Myr period.

These authors found that the shape of the resulting cluster formation history matches that of the field-star formation history based on CMD analysis very well for the past 10^9 yr (cf. their fig. 8). The absolute value for the star formation rate based on their most massive cluster analysis also matches that of the field stars, while the absolute values differ systematically for the results based on the total mass in star clusters; this is interpreted in terms of either a low-bound star cluster formation efficiency or a high degree of infant mortality. Once again, therefore, these results based on empirical cluster age distributions are affected by a degeneracy between cluster formation and disruption scenarios.

The precise shape of the most recent LMC cluster formation history derived by Maschberger & Kroupa (2011) depends ultimately on whether or not the actively star-forming region centred on 30 Doradus (30 Dor) and its massive central cluster R136 are included in the models. The Hunter et al. (2003) catalogue does not contain the 30 Dor region (see also the discussion in Section 6.2). Maschberger & Kroupa (2011, their figs 3, bottom, and 4) show that the LMC's cluster formation rate over the past $\sim$1 Gyr has remained constant within $\sim$10 per cent if 30 Dor is included, while it shows a reduction in the cluster formation rate in the past few $\times$ 10^7 yr by a factor of 3–4 if 30 Dor is not included. The cluster formation history based on the total mass in clusters shows a relatively enhanced period of cluster formation 20–40 Myr ago, and a reduction by a factor of $\sim$3–4 more recently (cf. their figs 5 and 6). Fig. 4 of Baumgardt et al. (2013), which shows the LMC cluster system in the ($\mathrm{d}N_{\rm cl}/\mathrm{d}t$ versus $\log t$) plane, also supports this conclusion.

In summary, although the LMC's cluster formation history is still subject to sizeable uncertainties, our null hypothesis of a roughly constant cluster formation rate for the past 10^9 yr is likely not too far off the mark. There is little, if any, modern empirical support for a significantly enhanced cluster formation rate in the past few $\times$ 10^7 yr, by an order of magnitude or more, which would be required to reconcile a high infant mortality rate with the results from our diagnostic tests in this paper, modulo the degeneracy

between cluster formation and disruption scenarios pointed out above. If anything, the galaxy's cluster formation rate may have declined by a factor of a few compared with that 20–40 Myr ago.

6.2 How representative is our LMC cluster data set?

Our results and the comparisons discussed in Sections 1 through 5 were largely based on the Hunter et al. (2003) cluster photometry of 748 distinct star clusters above a nominal selection limit of $M_V \simeq -4.3$ mag. To place these results into a more general context, we need to consider whether and to what extent this cluster data base is representative of the LMC's cluster population as a whole.

The Hunter et al. (2003) cluster sample is based on Massey's (2002) 14.5 deg^2 CCD survey of the Magellanic Clouds; for an overview of the survey's spatial coverage, see his fig. 1 (see also Maschberger & Kroupa 2011, their fig. 1). The Hunter et al. (2003) cluster sample does not cover the entire LMC (e.g. it does not cover the entire bar region), although this does not stop Hunter et al. (2003) from specifically assuming that their objects are representative of the LMC cluster population as a whole. Their data base covers approximately half of the LMC bar and a number of fields in the more extended LMC disc region. One important caveat is that the actively star-forming field centred on the 30 Dor region is not included in the catalogue. As we saw in Section 6.1, whether or not the young, massive clusters in this field are included in our analysis may lead to different interpretations as regards the shape of the cluster formation history.

Baumgardt et al. (2013, their fig. 1) show the coverage of the Hunter et al. (2003) clusters with respect to that of both the Pietrzyński & Udalski (2000, Optical Gravitational Lensing Experiment, OGLE II) and the Glatt et al. (2010) samples. The OGLE II sample predominantly covers the central regions of the galaxy, including the entire LMC bar. This sample thus extends the Hunter et al. (2003) coverage to include the missing part of the bar region, but it does not include a significant number of clusters in the more general field of the LMC. The Glatt et al. (2010) data are based on the MCPS, which covers the central 64 deg^2 of the LMC. Their clusters extend well beyond the coverage of the Hunter et al. (2003) data base, with a particularly large excess of clusters towards the north compared to the Hunter et al. (2003) coverage. Glatt et al. (2010) found evidence of variable star (cluster) formation histories across the LMC system, so that a complete picture of the galaxy's cluster properties requires the largest possible spatial coverage.

In the context of our focus on the youngest clusters in the LMC, it is therefore particularly frustrating that the Glatt et al. (2010) sample cannot shed light on the cluster formation and disruption scenarios for clusters younger than a few $\times$ 10^7 yr (cf. the discussion in Section 2). Nevertheless, these authors state specifically that 'the youngest clusters reside in the supergiant shells, giant shells, the intershell regions and towards regions with a high Hα content'. These regions, in particular the (super)giant shells as well as the young, star-forming blue and south-eastern arms, are mostly located outside the Massey (2002) survey area. However, in Fig. 5 we compared the Glatt et al. (2010) cluster parameters with those of de Grijs & Anders (2006) and Popescu et al. (2012), *for the same limiting magnitude*, and concluded that the d$N_{\rm cl}$/dt distributions as a function of age are both qualitatively and quantitatively similar for all samples. Since adoption of a limiting magnitude is equivalent to imposing a limiting mass for a given age, this leads us to suggest that the Hunter et al. (2003) clusters – which, after all, formed the basis for the de Grijs & Anders (2006) and Popescu et al. (2012) results – are representative of the LMC's cluster population

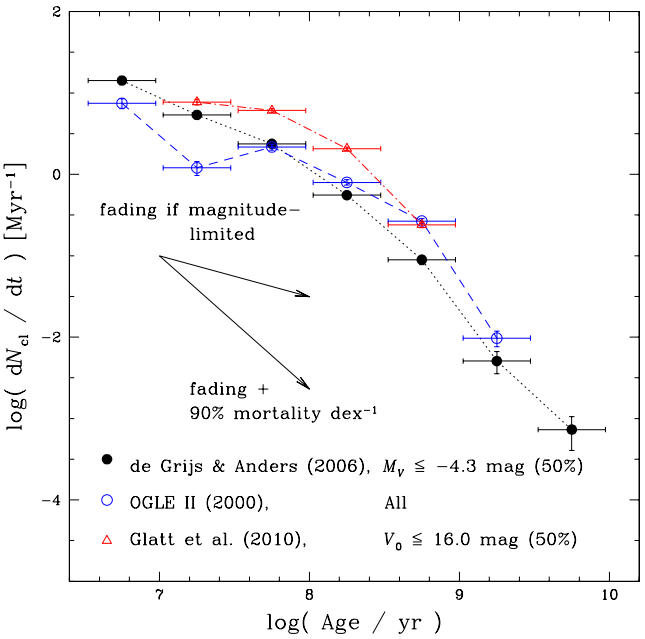

Figure 10. As Fig. 5, but for the OGLE II and Glatt et al. (2010) catalogues. The distributions include all clusters in the Pietrzyński & Udalski (2000) data base of cluster ages based on OGLE II and objects brighter than $V_0 = 16.0$ mag from the Glatt et al. (2010) sample, corresponding to the approximate 50 per cent completeness limit. The de Grijs & Anders (2006) results, for $M_V \leq -4.3$ mag, are shown for reference.

at large *for an age-dependent minimum mass limit* corresponding to $M_V \simeq -4.3$ mag. In other words, many of the young clusters in the Glatt et al. (2010) catalogue would fall below our selection limit adopted here (see below). These results also suggest that, although the Massey (2002) survey did not cover the entire LMC disc region, its coverage is sufficient to trace a representative, magnitude (mass)-limited sample of LMC clusters with ages up to 1 Gyr.

The diversity of cluster formation rates across the LMC (cf. Glatt et al. 2010) is exemplified by the d$N_{\rm cl}$/dt distributions in Fig. 10. We show the de Grijs & Anders (2006) results for $M_V \leq -4.3$ mag for reference. We also include the Glatt et al. (2010) clusters, having imposed a limiting magnitude of $V_0 = 16.0$ mag, which corresponds to their cluster sample's approximate 50 per cent completeness limit, if we assume that the bright end of the cluster luminosity function is adequately represented by a single power law. This sample of clusters has been drawn from across the extended LMC system, containing numerous clusters outside the Massey (2002) fields (cf. Baumgardt et al. 2013, their fig. 1). In addition, we show the distribution for the OGLE II clusters centred on the LMC bar with isochrone-based age determinations from Pietrzyński & Udalski (2000). The latter sample is limited to clusters younger than about 1.2 Gyr because of the observational completeness limit for single stars, $V \approx 21.5$ mag. The catalogue's photometric completeness characteristics have not been explored in detail (cf. Pietrzyński et al. 1999), but the depth of the observations is on the order of 1.5 mag shallower than that of the MCPS used by Glatt et al. (2010).

The differences in the cluster formation (and, possibly, disruption) histories among the three samples are clear. The Glatt et al. (2010) extended LMC disc sample contains a significantly larger sample of clusters at any age than the reference sample, but particularly for log (t yr^{-1}) $\gtrsim$ 7.5. Note, however, that the curve turns down

to lower rates more rapidly for younger ages than that representing the de Grijs & Anders (2006) sample. The OGLE II sample shows larger variations from one time step to the next, which may imply a significantly more bursty cluster formation rate in the galaxy's bar (cf. Pietrzyński & Udalski 2000) than in the less dense regions at larger radii sampled by both comparison samples. The overall trend, however, does not support a significant increase of cluster formation at very young ages.

Finally, we return to the obvious omission of the 30 Doradus region and its massive, central star cluster R136. This is one of a very small number of massive clusters left out of our analysis and which would have been taken into account given the observational selection limit imposed if it had been covered by the original survey data. Addition of a single or a few young, $<10^7$-yr-old clusters to either of our main data bases would increase the relevant number of clusters in this age range by $\sim$10–20 per cent. However, we would need at least an order of magnitude more young clusters and a factor of 2–4 more clusters with ages of $\log(t\,\mathrm{yr}^{-1}) \sim 7.5$ (and more massive than our age-dependent mass limit) to conclusively support a high degree of early cluster disruption. The empirical data do not allow us to reach such a conclusion.

7 CONCLUSION

On their own, the results based on any of the individual approaches presented here are merely indicative of the physical conditions governing the LMC's cluster population. However, the combination of our results from all three different diagnostics leaves little room for any conclusion other than that a high rate of early cluster disruption is summarily ruled out. The CDF results show, in particular, that high levels of infant mortality require that the vast majority of one's cluster sample must be young, unless the cluster formation rate would be significantly higher: for a disruption rate of 90 per cent per decade in age up to 10^9 yr, instead of the observed fraction of $<$15 per cent, more than half of our sample clusters would need to be younger than 10 Myr. Such high star and cluster formation rates appear to be ruled out for $t \lesssim 10^9$ yr on the basis of analyses of both the cluster population (Maschberger & Kroupa 2011) and the LMC field's star formation history (e.g. Harris & Zaritsky 2009; Rubele et al. 2012, and references therein).

We thus conclude that the cluster disruption rate in the LMC, at least over the past 100 Myr, has been well below that found for large and/or interacting galaxies like the Antennae system (Whitmore, Chandar & Fall 2007, and references therein), M51 (Bastian et al. 2005) and the Milky Way (Lada & Lada 2003). We do not find any compelling evidence of significant cluster disruption and estimate a conservative maximum disruption rate of less than 10 per cent per decade in $\log(t\,\mathrm{yr}^{-1})$, up to $t \simeq 10^8$ yr. It seems, therefore, that the difference in environmental conditions in the Magellanic Clouds on the one hand and significantly more massive galaxies on the other may be the key to understanding the apparent variations in cluster disruption behaviour.

ACKNOWLEDGEMENTS

We thank Holger Baumgardt and the referee for helpful contributions and suggestions, respectively. RdG and PA acknowledge research support through grant 11073001 from the National Natural Science Foundation of China (NSFC). This research has made use of NASA's Astrophysics Data System Abstract Service.

REFERENCES

Anders P., de Grijs R., Fritze-v A. U., Bissantz N., 2004a, MNRAS, 347, 17
Anders P., Bissantz N., Fritze-v A. U., de Grijs R., 2004b, MNRAS, 347, 196
Anders P., Kotulla R., de Grijs R., Wicker J. E., 2013, ApJ, submitted
Barker S., de Grijs R., Cerviño M., 2008, A&A, 484, 711
Bastian N., Gieles M., Lamers H. J. G. L. M., Scheepmaker R. A., de Grijs R., 2005, A&A, 431, 905
Bastian N. et al., 2012, MNRAS, 419, 2606
Baumgardt H., Parmentier G., Anders P., Grebel E. K., 2013, MNRAS, 430, 676
Bica E., Clariá J. J., Dottori H., Santos J. F. C., Jr, Piatti A. E., 1996, ApJS, 102, 57
Bica E., Bonatto C., Dutra C. M., Santos J. F. C., Jr, 2008, MNRAS, 389, 678
Boutloukos S. G., Lamers H. J. G. L. M., 2003, MNRAS, 338, 717
Bruzual A. G., Charlot S., 2003, MNRAS, 344, 1000
Cerviño M., Luridiana V., 2004, A&A, 413, 145
Cerviño M., Luridiana V., 2006, A&A, 451, 475
Cerviño M., Luridiana V., Castander F. J., 2000, A&A, 360, L5
Cerviño M., Valls-Gabaud D., Luridiana V., Mas-Hesse J. M., 2002, A&A, 381, 51
Cezario E., Coelho P. R. T., Alves-Brito A., Forbes D. A., Brodie J. P., 2013, A&A, 549, A60
Chandar R., Fall S. M., Whitmore B. C., 2006, ApJ, 650, L111
Chandar R., Fall S. M., Whitmore B. C., 2010a, ApJ, 711, 1263
Chandar R., Whitmore B. C., Fall S. M., 2010b, ApJ, 713, 1343
Colucci J. E., Bernstein R. A., 2012, ApJ, 749, 124
de Grijs R., Anders P., 2006, MNRAS, 366, 295
de Grijs R., Goodwin S. P., 2008, MNRAS, 383, 1000
de Grijs R., Goodwin S. P., 2009, in van Loon J. T., Oliveira J. M., eds, Proc. IAU Symp. 256, The Magellanic System: Stars, Gas, and Galaxies. Cambridge Univ. Press, Cambridge, p. 311
de Grijs R., Anders P., Bastian N., Lynds R., Lamers H. J. G. L. M., O'Neil E. J., 2003, MNRAS, 343, 1285
de Grijs R., Anders P., Lamers H. J. G. L. M., Bastian N., Fritze-v A. U., Parmentier G., Sharina M. E., Yi S., 2005, MNRAS, 359, 874
de Grijs R., Anders P., Zackrisson E., Östlin G., 2013, MNRAS, 431, 2917
de Meulenaer P., Narbutis D., Mineikis T., Vansevičius V., 2013, A&A, 550, A20
Fall S. M., Chandar R., 2012, ApJ, 752, 96
Fitzpatrick E. L., 1999, PASP, 111, 63
Fouesneau M., Lançon A., 2010, A&A, 521, A22
Fouesneau M., Lançon A., Chandar R., Whitmore B. C., 2012, ApJ, 750, 60
Geha M. C. et al., 1998, AJ, 115, 1045
Gieles M., Lamers H. J. G. L. M., Portegies Zwart S. F., 2007, ApJ, 668, 268
Girardi L., Chiosi C., Bertelli G., Bressan A., 1995, A&A, 298, 87
Glatt K., Grebel E. K., Koch A., 2010, A&A, 517, A50
Harris J., Zaritsky D., 2009, AJ, 138, 1243
Hunter D. A., Elmegreen B. G., Dupuy T. J., Mortonson M., 2003, AJ, 126, 1836
Kotulla R., Fritze U., Weilbacher P., Anders P., 2009, MNRAS, 396, 462
Kroupa P., 2002, Sci, 295, 82
Lada C. J., Lada E. A., 2003, ARA&A, 41, 57
Lamers H. J. G. L. M., 2009, Ap&SS, 324, 183
Lamers H. J. G. L. M., Gieles M., Bastian N., Baumgardt H., Kharchenko N. V., Portegies Zwart S., 2005, A&A, 441, 117
Maíz Apellániz J., 2009, Ap&SS, 324, 95
Maschberger T., Kroupa P., 2007, MNRAS, 379, 34
Maschberger T., Kroupa P., 2011, MNRAS, 411, 1495
Massey P., 2002, ApJS, 141, 81
Olszewski E. W., Suntzeff N. B., Mateo M., 1996, ARA&A, 34, 511
Parmentier G., de Grijs R., 2008, MNRAS, 383, 1103

Pietrzyński G., Udalski A., 2000, Acta Astron., 50, 337
Pietrzyński G., Udalski A., Kubiak M., Szymański M., Woźniak P., Żebruń K., 1999, Acta Astron., 49, 521
Popescu B., Hanson M. M., 2010, ApJ, 724, 296
Popescu B., Hanson M. M., Elmegreen B. G., 2012, ApJ, 751, 122
Portegies Zwart S. F., McMillan S. L. W., Gieles M., 2010, ARA&A, 48, 431
Rafelski M., Zaritsky D., 2005, AJ, 129, 2701
Rubele S. et al., 2012, A&A, 537, A106
Salpeter E. E., 1955, ApJ, 121, 161
Sarajedini A., 1998, AJ, 116, 738
Silva-Villa E., Larsen S. S., 2010, A&A, 516, A10
Silva-Villa E., Larsen S. S., 2011, A&A, 529, A25
Whitmore B. C., Chandar R., Fall S. M., 2007, AJ, 133, 1067
Zaritsky D., Harris J., Thompson I. B., Grebel E. K., 2004, AJ, 128, 1606

SUPPORTING INFORMATION

Additional Supporting Information may be found in the online version of this article:

Table 1. LMC cluster positions and derived parameters (http://mnras.oxfordjournals.org/lookup/suppl/doi:10.1093/mnras/stt1541/-/DC1).

Please note: Oxford University Press is not responsible for the content or functionality of any supporting materials supplied by the authors. Any queries (other than missing material) should be directed to the corresponding author for the paper.

This paper has been typeset from a TEX/LATEX file prepared by the author.